

# A Generalized Dynamic Planning Framework for Green UAV-Assisted Intelligent Transportation System Infrastructure

Michael C. Lucic, *Student Member, IEEE*, Hakim Ghazzai<sup>✉</sup>, *Member, IEEE*, and Yehia Massoud, *Fellow, IEEE*

**Abstract**—Roadside unit (RSU) planning is vital for the operation of an intelligent transportation system (ITS). RSUs provide ground coverage limited by obstacles. Unmanned aerial vehicles (UAVs) can complement RSU coverage by providing flexible connectivity capable of adapting coverage for traffic fluctuations, energy consumption, and budgetary constraints that all have effects on ITS operations. This article proposes a general RSU/UAV joint planning solution, where complex dynamic parameters are investigated. The objective is to maximize the effective coverage of placed RSUs and UAV docks given: a budget comprised of periodic operating expenses and capital expenditures, limitations of the ground transceivers and UAVs, and use of renewable energy to offset the on-grid electricity cost. We formulate a mixed-integer quadratically constrained problem that can determine the optimal placement of RSUs and UAV stations, RSU activation schedules, if solar panels are attached, and their coverage during each time period. Due to NP-hard complexity of such a planning problem, we design a heuristic algorithm that produces suboptimal solutions in less time. Afterward, we perform a sensitivity analysis and show that changes to the parameters lead to logical shifts in infrastructure coverage. Additionally, we visualize the algorithm’s performance on a large setting—Manhattan Island.

**Index Terms**—Infrastructure planning, intelligent transportation systems (ITSs), roadside unit (RSU), unmanned aerial vehicle (UAV).

## I. INTRODUCTION

OVER the past decade, there has been an increasing interest in connected/autonomous vehicle development, incorporating more devices into the Internet of things, and leveraging the ever-growing user data into useful action plans. The new autonomous and connected vehicles have a whole suite of new technologies [2]. These new features, paired with new high-speed connections to the Internet and new data-processing methods, can be utilized to provide more detailed, accurate, and useful real-time information that can be invaluable for intelligent transportation system (ITS) end-users. The ITS has the capability of leveraging these data for safer and more reliable transportation systems [3], [4].

Manuscript received July 11, 2019; revised October 4, 2019 and January 17, 2020; accepted January 20, 2020. Date of publication February 17, 2020; date of current version November 24, 2020. This article was presented in part at the IEEE International Systems Conference, Orlando, FL, USA, Apr. 2019 [1]. (*Corresponding author: Hakim Ghazzai*.)

The authors are with the School of Systems and Enterprises, Stevens Institute of Technology, Hoboken, NJ 07030 USA (e-mail: mlucic@stevens.edu; hghazzai@stevens.edu; ymassoud@stevens.edu).

Digital Object Identifier 10.1109/JSYST.2020.2969372

Roadside units (RSUs) stand to serve as the main infrastructure backbone of an ITS—they will likely serve as the main connection gateway for smart vehicles. RSUs face a number of challenges in practice, due to their placement around ground level. One example is seamless communication issues—RSUs may have channel interruptions from other radio signals and obstacles. Moreover, RSUs are relatively expensive to deploy, due to high installation, i.e., capital expenditures (CAPEX), as well as relatively high operational and maintenance costs, i.e., operational expenditure (OPEX).

While RSUs serve to work as the main piece of ITS communication infrastructure, UAVs stand to fill a role of providing the network flexibility—they may provide better communication links than RSUs and cover areas that either lack RSU coverage due to location or are experiencing an unusual amount of demand. UAV considerations in the ITS are a new concept, and as a result, there are not many systems that plan or schedule UAVs in ITS applications, and even less that also consider them in concert with RSU planning [5].

There are many application possibilities for RSUs in the ITS, including, but not limited to, traffic flow control [6], social network behavior analysis in vehicular social networks (VSNs) [7], and connecting untrusted parties [8]. All of these applications are examples of how RSUs may be applied in ITS applications. Many other applications, such as [2], highlight the importance of RSUs in ITS-based systems, like VSNs, mainly through their ability to act as a communication gateway for Internet connectivity for smart vehicles.

ITS planners face several challenges when it comes to figuring out how to build a robust network of infrastructure involving heterogeneous ITS components, i.e., RSUs and UAVs. First, RSUs only have a limited effective range [9], which is further effected by transmission channel loss [10]. Second, UAVs are also limited by range due to two primary factors [5]: 1) battery power—UAVs must charge, act, and then return to their bay station prior to reuse, leading to them, only being available in a temporary capacity; and 2) on-board transmitter range—the short-range transmitter connected to the UAV has a smaller effective communication range, limited by similar factors as the limited range of the RSU transmitters. Third, there is a finite (and likely small) amount of financial resources that can be budgeted for the RSU/UAV station installation and operations. Fourth, both efficient energy consumption and varying traffic flow through certain areas need to be considered in tandem. For instance, it is preferable to place RSUs in areas with higher volumes of traffic, so larger amounts of data can be sent through the ITS infrastructure and returned to the vehicles, or to place RSUs in areas requiring higher monitoring levels to report

incidents. UAV stations have a little more flexibility and may be more useful in cases where the traffic flow variation fluctuates more wildly. During periods of low traffic, RSUs in less busy areas can be switched OFF to conserve energy and then switched back ON to cope with increased network demand, and UAVs can remain docked, active, or move to other stations to match demand fluctuations. An effective planning problem will go beyond static installation by considering temporal variations in traffic conditions (e.g., periodic and stationary process, where, for example, there is rush-hour traffic daily at 5:30 P.M. every day, leading to higher roadway utilization at that time) to ensure that RSUs and UAV stations are installed in optimal locations for the whole day and also can switch RSUs ON or OFF automatically to match time-dependent traffic behavior changes across different time periods.

As far as the authors know, this article proposes a novel and generic approach to optimally plan, install, and schedule RSU and UAV infrastructure for ITS applications. The objective of this approach is to place RSUs and UAV stations in such a way to maximize the effective coverage of the transceiver/UAV network (configuring them to cover the most important areas reflected by a fitness utility metric, given the budgetary restrictions, tradeoffs between installation costs versus operational costs, physical limitations of the transmitters, local realistic topology of the area of interest, factoring in renewable energy sources, specifically solar power, which can offset emissions and also reduce OPEX, and considering the differences in RSU coverage versus UAV coverage). Solar panels will incur additional installation costs, which need to be factored into budgetary considerations as well.

Considering the aforementioned factors, we have the following.

- 1) We formulate a mixed-integer quadratically constrained program (MIQCP) to provide a guide for ITS planners on the optimal installation locations of RSUs, UAVs, and solar panels, the daily schedule of activating/deactivating RSUs, the number of UAVs associated with each station, the range of the RSUs at each time period, and the financial resources required to implement the solution. The developed model readily solves the ITS planning problem for all given financial parameters.
- 2) We develop a heuristic for faster solutions with the goal of maximizing coverage efficiency while remaining within the budget and respecting the other model constraints in an iterative manner. Our development of the heuristic is motivated by the fact that the MIQCP solution time is quite slow due to the NP-hard complexity of the methods required to solve it. The heuristic algorithm developed in this article finds suboptimal solutions approximately 5–10% worse than the optimal solution in a dramatically shorter period of time (hundreds to thousands of times faster) than the state-of-the-art solver used as a benchmark.
- 3) We design the framework to work for any realistic road network, unlike previous work considering simplified grids, or one-dimensional road networks. The other models consider either installation or scheduling separately; this framework considers both at the same time. Additionally, our model considers budget, traffic flow, temporal changes, physical device limitations, and renewable energy all at once, rather than considering one or two of these factors separately.

In this article, Section II contains a treatment of literature related to the scope of our problem. Section III discusses the

development of the system model. Section IV describes the formulation of the optimization model. Section V focuses on the development of the fast heuristic algorithm. Section VI discusses the findings and sensitivity analysis of the models. Finally, Section VII concludes this article.

## II. LITERATURE REVIEW

In this section, we first review the technologies incorporated in our planning problem and how previous researchers have worked to plan the placement and scheduling of ITS infrastructure, as these approaches are put together in a larger framework in the following sections.

Vehicles in future transportation settings will be armed with a wide array of sensor technologies that may be used for data collection and transmission. The interconnectivity of future vehicles will lead to the use of VSNs to leverage the increased volume of data for improving the reliability and operation of the ITS [2]. In order to facilitate robust connectivity, a central infrastructure comprised of RSU serves as the core gateway for smart vehicle connectivity for data collection and transmission. In special cases where there is no coverage from the central infrastructure, and the vehicles are far enough where vehicle to vehicle hops are infeasible or too slow, UAVs may fill roles to improve connectivity in sparse areas, ensuring maximal connectivity.

The most commonly proposed infrastructure development by researchers is to install RSUs alongside the roadways [9]. These short-range transceivers allow for a sufficiently fast data transmission rate between the infrastructure and vehicles passing through its effective range, so all relevant data can automatically be forwarded to the main control system and *vice versa*. Many ITS applications, such as the electric vehicle charging scheme developed in [11], depend on the operation of RSUs as a central piece of the infrastructure.

As mentioned in the introduction, there are many challenges associated with RSU planning. Previous work has looked at each of the aforementioned challenges from the introduction in isolation, or in less complex settings. In [12], the approach to optimal placement was to formulate the problem as an integer programming Knapsack problem, with the objective to maximize coverage by deciding whether or not to place RSUs, given a set of candidate locations and budget constraints. The authors of [13] designed an RSU placement scheme utilizing movement patterns, rather than analyzing specific trajectories, providing the basis for utilizing a fitness metric to guide placement. In [14], the authors investigated how network performance relates to the effectiveness of coverage (e.g., focusing placement in more useful locations), which provides further justification for the objective selection in our model. The authors of [15] utilized multiobjective approaches to factoring both capital (a.k.a. CAPEX) and operational (a.k.a. OPEX) expenditures and the tradeoff between both for placement in the minimization of cost for RSU placement. Finally, in [16], the authors discussed energy-efficient RSU scheduling and placement. Their approach led to the combined installation and scheduling of RSUs, another factor incorporated into the proposed framework.

The authors of [17] develop a genetic evolutionary algorithm for RSU planning, showing the motivation for a fast solver for complex RSU planning. A genetic algorithm is not applicable for our problem, because the work in [17] considers a much

simpler problem space with no constraints and preselected RSU locations.

Other potential ITS infrastructure research has centered around utilizing UAV technology [18]. UAVs have the advantage of more direct links with ground terminals, due to their elevated position, as well as being able to quickly change location to accommodate rapid developments in transportation system behavior—RSUs provide fixed-location service, where the UAV can dynamically shift coverage based on changes in the system. Our approach was to blend all of these factors into a singular framework to aid ITS decision makers when installing/scheduling RSUs. Researchers have considered many potential applications of UAVs in ITS, including, but not limited to, monitoring traffic [19], utilizing UAV-based monitoring for prediction of traffic flow volume [20], acting as a vehicular ad hoc network transmission relay [21], as a mobile airborne transmission base station to improve connectivity where there is sparse permanent infrastructure development [22], and for data collection from remote RSUs [23].

The authors of both [24] and [25] develop multiple heuristic approaches to the placement of UAV stations to maximize effective coverage of a road network. UAV station placement runs in a similar vein to RSU placement, especially given the formulation and solution approach presented. The authors of [26] and [27] develop frameworks for managing the behavior of UAVs for data collection and mission scheduling, respectively. The authors of [28] develop a method for management and deployment of UAVs for surveillance applications. We assume that with the placement of UAV stations, systems like the ones discussed in these two papers, will manage the operations of UAVs in real time.

In our previous work [1], we developed a framework for the placement and scheduling of just RSUs. In this article, we incorporate the operation of UAVs within our previously developed framework in order to consider the two most popular infrastructure choices for ITS systems in one unified heterogeneous framework. The scope of our problem pertains to the planning of RSU and UAV infrastructure for ITS planning in future smart cities.

### III. SYSTEM MODEL

We consider a complex road network consisting of  $K = |\Phi|$  geographic coordinates (e.g., points), where  $\Phi$  is the set of points in the area of interest, and  $|\Phi|$  represents the cardinality of the set (i.e., the number of points considered). These points can either be intersections or along segments of roadways between intersections (see Fig. 1). The points are identified by their geographic coordinates, and each is characterized by a fitness metric score  $f_k$  assigned by the ITS planner, where  $k = 1, 2, \dots, K$ ,  $k \in \Phi$  denotes the index of each unique point on the map. This fitness metric is calculated by utilizing a weighted additive utility function considering the traffic flow density, accident rate, and/or other various factors pertinent to a traffic system. Our model also considers time-dependent variation in the fitness scores based on traffic flow changes, such as during rush hour, late-night periods, etc. To account for this, we add the index  $t$  to consider spatiotemporal fitness scores  $f_{kt}$  during time period  $t = 1, 2, \dots, |\mathcal{T}|$ , where  $\mathcal{T}$  represents the set of time periods in the day, and each time period is  $\frac{24}{|\mathcal{T}|}$  h in duration.

Our model considers a set of points  $\mathcal{J}$  that are candidate RSU/UAV station installation locations, preselected by the ITS

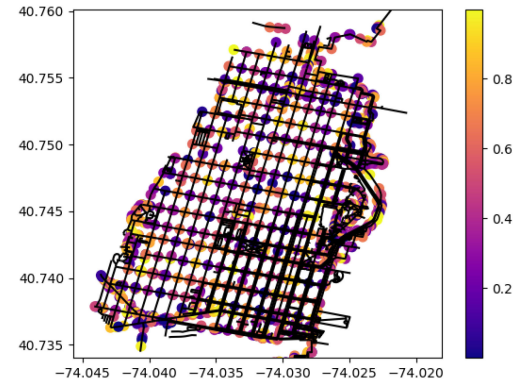


Fig. 1. Road network of Hoboken, NJ, which was utilized to test the model's behavior. The color bar  $([0, 1])$  represents a normalized utility function representing a linear combination of various factors, including traffic flow density, accident rate, and other factors that determine how "important" a point is. The black lines are the city's roads.

planners based on geological, topographical, and right-of-way restrictions. The ITS planners have a set of unique RSU classes  $\mathcal{I}$ , where  $i = 1, 2, \dots, |\mathcal{I}|$ , that they may choose from to install. These different RSU classes each have unique characteristics such as effective range, power consumption, installation costs, etc.

We consider the possibility of installing photovoltaic solar panels at each RSU or UAV station that can be used to offset the consumption of electricity from the conventional power grid. We consider that the number of RSUs, UAV stations, and solar panels installed by the ITS operator is dependent on maximizing the utilization of a daily operating budget denoted by  $\bar{D}$ ; this periodic budget includes i) OPEX such as electricity, denoted by  $\gamma$ , and ii) periodic amortized CAPEX of installing RSUs of type  $i$ , UAV stations, and solar panels denoted by  $c_{ir}$ ,  $c_d$ , and  $c_{sq}$ , respectively, where  $q \in \Omega$ ,  $q = 1, 2, \dots, |\Omega|$ , represents different classes of solar panels in the same vein as the different classes  $\mathcal{I}$  of RSUs.

#### A. RSU Power Consumption Model

We assume that the power consumption of the RSU of type  $i$  placed at point  $j$  and activated at time period  $t$  is expressed as follows [29]:

$$P_{ijt}^{\text{tot}} = a_i p_{ijt} + b_i \quad (1)$$

where  $a_i$  is the ratio between transmission power and required power to amplify the signal and  $b_i$  is energy converted to heat by electrical resistance.<sup>1</sup> The variable  $p_{ijt}$  is the transmission power of an RSU of type  $i$  placed at a location  $j$  during time period  $t$ . Its value cannot exceed the maximum power rating, denoted by  $P_i^{\max}$ , as follows  $p_{ijt} \leq P_i^{\max}$ .

#### B. RSU Coverage Model

In our model, we assume that a point  $k$  is being covered by an RSU placed at point  $j$  if the distance between the two points is less than the range of the transmitter being able to transmit data at a desired throughput  $R$ , in Mb/s. We derive the RSU range using

<sup>1</sup> Assuming a linear model for the power model has been considered in many previous studies as it approximates the power consumption and reasonably approximates the analyses [29] and [30].

the channel power loss model [31]. After careful mathematical manipulations, the effective distance threshold  $d_{\text{th}}$  in meters to have a minimum data transfer rate  $R$  given a transmission power  $p_{\text{th}}$  in Watts is given as follows:

$$d_{\text{th}} = 10^{\left(\frac{-PL_0}{10\nu}\right)} \left[ \frac{p_{\text{th}}}{K_b T B \left[ 2^{\left(\frac{R}{B}\right)} - 1 \right]} \right]^{\frac{1}{\nu}} \quad (2)$$

where  $PL_0$  represents the initial power loss in dBm,  $\nu$  is the dimensionless path loss exponent,  $K_b$  is Boltzmann's constant,  $T$  is the blackbody radiation temperature in Kelvin, and  $B$  is the bandwidth in MHz. We manipulate the equation to find the power transmission threshold  $p_{\text{th}}(j, k, R)$ , defined as the minimum transmission power required to achieve a data transfer rate  $R$  given the distance between points  $j$  and  $k$ ,  $d_{\text{th}}(j, k)$ :

$$p_{\text{th}}(j, k, R) \geq \left( K_b T B \left[ 2^{\left(\frac{R}{B}\right)} - 1 \right] \right) \left( d_{\text{th}}(j, k) \left[ 10^{\left(\frac{PL_0}{10\nu}\right)} \right] \right)^{\nu}. \quad (3)$$

### C. UAV Power Consumption Model

We assume that the power consumption of a UAV station with  $N$  UAVs installed at location  $j$  and active at time period  $t$  is expressed as follows:

$$P_{jt}^{\text{tot}}(N) = C_T p^{\text{use}} N \quad (4)$$

where  $C_T$  is the fraction of time in the UAV operations spent charging (e.g., if a UAV spends 20 min of an hour of operation charging,  $C_T = \frac{20}{60} = 0.33$ ), and  $p^{\text{use}}$  is the power (in Watts) required to charge a UAV. The UAV power parameter  $p^{\text{use}}$  corresponds to the average power consumption of the UAV. We consider average statistics for the UAV power consumption, as the aim of our model is to develop a long-term planning framework. This value can be set to average consumption, consumption based on worst-case UAV operation factors, etc., based on the preferences of the system operator.

### D. UAV Coverage Model

The authors of [25] developed a model of the range of a UAV station based on the battery life of a UAV. In order to generalize the problem, we assume a fixed range radius  $\delta$  of a UAV station, where it is possible for a UAV to cover during that time period—this radius, for example, can be derived from [25, eqs. (12) and (14)]. Recall that we are proceeding with a proactive planning solution, where RSU and UAV station placement is based on average statistics of the road network. Therefore, we assume that the UAV itself has a smaller range of actual coverage ( $r_d$ ) that is a subset of the area covered by the station ( $A_T = \pi\delta^2$ ), based on the channel loss of the UAV's transmitter unit [31]. Knowing a UAV has a coverage area of  $A_d = \pi r_d^2$ , we can assume that the fraction of UAV covering an area of interest within the UAV station area of coverage is  $\frac{A_d}{A_T}$ , so the fraction of an area being covered with  $n$  UAVs is

$$\pi_{\text{cov}} \approx n \frac{A_d}{A_T}. \quad (5)$$

### E. Solar Power Model

The maximum amount of power generated from a solar panel of type  $q$  can be expressed as follows [32]:

$$\phi_q^{\max} = A_q \Psi \eta \quad (6)$$

where  $A_q$  represents the surface area of the solar panel of type  $q$  in  $\text{m}^2$ ,  $\Psi$  represents the maximum solar radiance in  $\text{W/m}^2$ , and  $\eta$  represents the efficiency of the solar panel. The parameters  $\Psi$  and  $\eta$  are constants in our model predefined by the user and can capture different aspects such as weather conditions and solar panel specifications. In our model,  $\bar{\theta}_{qt}$  represents the average solar power generated during time period  $t$  and can be calculated by the following formula [32]:

$$\bar{\theta}_{qt} = \frac{\phi_q^{\max} e^{-(\tau_t - \mu_\tau)^2}}{\sigma_\tau^2} \delta_t \quad (7)$$

where  $\tau_t$  represents the middle time of the time period (e.g., if the time period goes from 12 P.M. to 4 P.M.,  $\tau_t = 2$  P.M.),  $\mu_\tau$  represents the time of day that the peak power generation occurs (e.g., 12 P.M.),  $\sigma_\tau$  represents the half-width of half of the peak (e.g., 3 h), and  $\delta_t$  represents the duration of the time period  $t$  in hours.<sup>2</sup>

## IV. PROBLEM FORMULATION

In this section, we formulate an optimization program with the goal of maximizing the effective daily coverage of the installed RSUs, while factoring in the previous considerations we made in Section III.

### A. Objective Function

Our objective is to install RSUs and UAV stations, schedule activation/deactivation of RSUs, and orchestrate the behavior of the UAV fleet optimally such that the coverage of the points on the map is maximized while remaining within the budget with respect to the unique fitness values of each point  $k$ . The daily coverage efficiency (%) is defined as

$$E = \frac{\sum_{k \in \Phi} \sum_{t \in \mathcal{T}} \Lambda_{kt} f_{kt}}{\sum_{k \in \Phi} \sum_{t \in \mathcal{T}} f_{kt}} \quad (8)$$

where  $\Lambda_{kt}$  is a continuous value in the inclusive range  $[0, 1]$  representing the normalized coverage of a point  $k$  during time period  $t$ ,  $\Lambda_{kt} = 1$  represents perfect coverage of the point (e.g., the point is covered always during the duration of the time period), ignoring noisy disturbances, and  $\Lambda_{kt} = 0$  represents the point not being covered at all. Fuzzy values of  $\Lambda_{kt}$  between 0 and 1 correspond to the fraction of time during the time period that the point is covered (e.g., if  $\Lambda_{kt} = 0.2$ , then point  $k$  is covered 20% of the duration of time period  $t$ ).

Another possibility to deal with such a planning problem is to factor in minimization of the budget as part of a multiobjective problem, rather than as a constraint for a problem with the above function as our single objective; we must consider a normalized cost function as part of our decision making. In the following

<sup>2</sup>Other solar and UAV power models existing in literature such as [26] can be used with this framework. Indeed, the developed framework can work with any power model and does not require a specific formulation as long as the average or worst-case (depending on the preferences of the planner) UAV speed and solar power generation is considered.

equations, we define the cost function  $B_c$  representing the amortized implementation and operational cost of the deployed infrastructure

$$B_c = \sum_{j \in \mathcal{J}} \sum_{t \in \mathcal{T}} \left( \sum_{i \in \mathcal{I}} (\Delta_{ijt} + \Omega_{ijt}) \right) (O_{jt} + C_{jt}) \quad (9)$$

where

$$\Delta_{ijt} = x_{ijt} \left( \max \left\{ \left( (a_i p_{ijt} + b_i) - \sum_{q \in \Omega} Q_{qj} \bar{\theta}_{qt} \right), 0 \right\} \right) \gamma \quad (10a)$$

$$\Omega_{ijt} = c_{ir} x_{ijt} \quad (10b)$$

$$O_{jt} = \eta_{jt} \left( \max \{ ((C_T p^{\text{use}} N_{jt}) \right. \quad (10c)$$

$$\left. - \sum_{q \in \Omega} Q_{qj} \bar{\theta}_{qt}), 0 \} \right) \gamma \quad (10d)$$

$$C_{jt} = c_d \eta_{jt} + \sum_{q \in \Omega} c_{sq} Q_{qj} \quad (10e)$$

where  $\Delta_{ijt}$  is the OPEX of an RSU of type  $i$ , placed at a location  $j$  during time slot  $t$  as a function of the RSU power consumption  $x_{ijt}(\max\{(a_i p_{ijt} + b_i) - \sum_{q \in \Omega} Q_{qj} \bar{\theta}_{qt}, 0\})\gamma$ , where  $\gamma$  represents electricity expenses. The parameter  $\Omega_{ijt}$  is the per-time-period amortized CAPEX of installing an RSU  $c_{ir} x_{ijt}$ . The parameter  $O_{jt}$  is the OPEX of a UAV station, dependent on the number of UAVs active at the station.  $C_{jt}$  is the amortized CAPEX of installing a UAV station ( $c_d \eta_{jt}$ ) and/or a solar panel  $c_{sq} Q_{qj}$ . We use the max function for the solar power offset to count only the on-grid electricity cost and avoid a situation, where the marginal OPEX makes the budget incrementally larger by taking negative values. In our code implementation, we linearize the max functions. We made the choice of the budget as a constraint based on the problem formulations in [12] and [34]. The multiobjective cost function, denoted by MOF, is therefore

$$\text{MOF} = \omega_p E - (1 - \omega_p) B_c \quad (11)$$

where  $\omega_p$  is the Pareto weight allowing the achievement of a certain tradeoff between the coverage efficiency  $E$  and the infrastructure budget  $B_c$ . Extreme values of  $\omega_p$  will lead to no infrastructure placement ( $\omega_p = 0$ ) or maximum infrastructure placement at maximum cost ( $\omega_p = 1$ ).

## B. Problem Constraints

Our goal of maximizing the coverage efficiency of the heterogeneous ITS infrastructure is constrained by the following.

1) *Coverage Constraints:* The coverage of point  $k$  at time period  $t$  is based on the following:

$$\Lambda_{kt} = \max \{ z_{kt}, \rho_{kt} \} \forall k, t \in \Phi, \mathcal{T} \quad (12)$$

where  $z_{kt}$  represents whether or not a point  $k$  is covered by an RSU at time period  $t$ , and  $\rho_{kt}$  represents the average effective coverage of a point  $k$  at time period  $t$  from a UAV station on a continuous range between  $[0, 1]$ , where 1 represents the maximum continuous coverage and 0 represents no coverage.

The RSU coverage  $z_{kt}$  is defined as

$$z_{kt} = \text{OR}_{i \in \mathcal{I}, j \in \mathcal{J}} (x_{ijt} y_{ijkt}) \forall k, t \in \Phi, \mathcal{T} \quad (13)$$

where point  $k$  is considered covered at time period  $t$  if there is at least one RSU of type  $i$  placed at point  $j$  activated during time  $t$  ( $x_{ijt} = 1$ ), and point  $k$  is within the effective transmission range of that RSU ( $y_{ijkt} = 1$ ) based on the coverage model highlighted in Section III-A. A logical  $\text{OR}_{i \in \mathcal{I}, j \in \mathcal{J}}$  function is used to prevent double counting of the point in the objective function (i.e., if the point rests within the transmission range of two or more different RSUs, it is only counted as covered once). We linearize this constraint in our code implementation.

The UAV station coverage is expressed as

$$\rho_{kt} = \frac{A_d}{A_T} \sigma_{kt} S_T \forall k, t \in \Phi, \mathcal{T} \quad (14a)$$

$$\sigma_{kt} = \max_j \{ \mu_{jkt} N_{jt} \} \forall k, t \in \Phi, \mathcal{T} \quad (14b)$$

where  $\frac{A_d}{A_T}$  is defined in Section III-D,  $S_T$  represents the fraction of UAV operational time dedicated to service (i.e., actually in flight or covering an event),  $N_b$  represents the maximum size of the entire UAV fleet, and  $\sigma_{kt}$  represents the maximum number of UAVs that may cover a point  $k$  during time period  $t$ . We linearize this constraint in our code implementation.

2) *RSU Range Constraints:* Elaborating further on the definition of a point  $k$  being within the RSU transmission range

$$y_{ijkt} = \begin{cases} 1, & \text{if } p_{ijt} x_{ijt} \geq p_{\text{th}}(j, k, R) \\ 0, & \text{otherwise.} \end{cases} \quad \forall i, j, k, t \in \mathcal{I}, \mathcal{J}, \Phi, \mathcal{T} \quad (15)$$

If the transmission power of an active RSU of type  $i$  located at point  $j$  during time period  $t$  is equal to or greater than the threshold  $p_{\text{th}}(j, k, R)$  defined earlier, point  $k$  is covered. We linearize this constraint in our code implementation through big-M reformulation. Also, point  $k$  can only be covered by an RSU type  $i$  placed/activated at a point  $j$  during time  $t$  if an RSU is active at point  $j$ ; this is guaranteed using the following constraint:

$$y_{ijkt} \leq x_{ijt} \forall i, j, k, t \in \mathcal{I}, \mathcal{J}, \Phi, \mathcal{T}. \quad (16)$$

3) *UAV Range Constraints:* In a similar vein to the definition of RSU coverage defined in (15), the coverage of point  $k$  from a UAV station active at location  $j$  and during time period  $t$  is defined as

$$\mu_{jkt} = \begin{cases} 1, & \text{if } \text{dist}(j, k) \leq \delta \eta_{jt} \\ 0, & \text{otherwise.} \end{cases} \quad \forall j, k, t \in \mathcal{J}, \Phi, \mathcal{T} \quad (17)$$

If the distance between points  $j$  and  $k$  is less than the radius of the range of the UAV station ( $\delta$ ), then point  $k$  is covered. Similarly to (12), we linearize this constraint in our code implementation through big-M reformulation. Additionally, point  $k$  cannot be covered by a UAV station at point  $j$  if one does not exist or is not active as indicated by the following constraint:

$$\mu_{jkt} \leq \eta_{jt} \forall j, k, t \in \mathcal{J}, \Phi, \mathcal{T}. \quad (18)$$

4) *RSU Specification Constraint:* The transmission power of an active RSU cannot exceed its maximum power rating as follows:

$$p_{ijt} \leq x_{ijt} P_i^{\text{max}} \forall i, j, t \in \mathcal{I}, \mathcal{J}, \mathcal{T}. \quad (19)$$

5) *Optional Budgetary Constraint*: If we utilize our single-objective function in the problem formulation (8), then the following budget constraint must be satisfied:

$$B_c \leq \bar{D} \quad (20)$$

where  $\bar{D}$  is the budget set by the ITS operator.

6) *Uniqueness Constraints*: To ensure uniqueness of RSU placement, at most only one RSU of type  $i$  can be placed at point  $j$  can be activated/installed at time period  $t$ , and UAV stations and RSUs shall not be located on the same point  $j$

$$\left( \sum_{i \in \mathcal{I}} x_{ijt} \right) + \eta_{jt} \leq 1 \forall j, t \in \mathcal{J}, \mathcal{T} \quad (21a)$$

$$\left( \sum_{j \in \mathcal{J}} x_{ijt} \right) \leq 1 \forall i, t \in \mathcal{I}, \mathcal{T}. \quad (21b)$$

Additionally, the number of scheduled UAVs cannot exceed the maximum fleet size  $N_b$

$$\sum_{j \in \mathcal{J}} N_{jt} \leq N_b \forall t \in \mathcal{T} \quad (22)$$

and the number of UAVs assigned to an active station located at point  $j$  during time period  $t$  cannot exceed the maximum number of UAVs needed to fully cover the effective range of the UAV station

$$N_{jt} \leq \frac{\eta_{jt}}{S_T \frac{A_d}{A_T}} \forall j, t \in \mathcal{J}, \mathcal{T}. \quad (23)$$

7) *Time Consistency Constraints*: To match demand fluctuations of traffic in the area, RSUs can be turned ON or OFF in order to further conserve electricity. One thing to keep in mind is that the time periods in  $T$  are *not* ordered chronologically; they are ordered in ascending order of overall network activity—rush-hour periods would likely be the highest indexed time periods, and late-night periods would likely be the lower indexed time periods, for example. Since we order the time periods from times with the least overall demand to most overall demand, the RSU active during less busy time periods must remain ON during busier time periods, and UAV station placement must be consistent across all time periods

$$x_{ijt} \leq x_{ij(t+1)} \forall i, j, t \in \mathcal{I}, \mathcal{J}, \mathcal{T} \setminus |\mathcal{T}| \quad (24a)$$

$$\eta_{jt} \leq \eta_{j(t+1)} \forall j, t \in \mathcal{J}, \mathcal{T} \setminus |\mathcal{T}|. \quad (24b)$$

After solving the problem, when time periods are reordered chronologically, the values of  $x_{ijt}$  form a daily schedule for RSU activation/deactivation. Note that this is a proactive ON/OFF switching planning of the RSUs. Real-time and instantaneous ON/OFF switching of RSUs can still be applied for the active RSUs depending on the instantaneous parameters of the road network.

8) *Solar Panel Consistency Constraints*: In this problem setting, solar panels may only be placed at locations, where an RSU or UAV station has been installed

$$q_{qj} \leq \sum_{t \in \mathcal{T}} \left( \eta_{jt} + \left( \sum_{i \in \mathcal{I}} x_{ijt} \right) \right) \forall j, q \in \mathcal{J}, \Omega \quad (25)$$

and only at most one solar panel may be placed at a location

$$\sum_{q \in \Omega} q_{qj} \leq 1 \forall j \in \mathcal{J}. \quad (26)$$

### C. Mixed-Integer Nonlinear Programming Formulation

Recall our objective formulated in Section IV-A; to maximize coverage efficiency and given all of the above constraints, the single-objective optimization program takes the following form:

$$\begin{aligned} & \max E \\ & \text{s.t. (10), (12)–(26)} \end{aligned}$$

and the multiobjective optimization program takes the form

$$\begin{aligned} & \max \text{MOF} \\ & \text{s.t. (10), (12)–(26) except (20).} \end{aligned}$$

These programs are mixed-integer nonlinear programs (MINLPs). The MINLP form is incredibly expensive computationally to solve, and no exact methods exist to optimally solve such a problem in a reasonable amount of time [33]. Therefore, we need to reformulate the problems in a different way in order to utilize an off-the-shelf solver software such as the Gurobi MIP solver to solve it optimally [35]. We reformulate the problems as MIQCPs, as the off-the-shelf solver can find the optimal solution for this type of problem utilizing techniques to minimize the candidate pool of solutions as a focused search, such as branch-and-bound, cutting planes, and model presolve [33]. Due to the high computational complexity of the state-of-the-art numerical methods required to solve an MIQCP formulation, we propose a greedy heuristic in Section V and, then, compare the performance of our heuristic and the state-of-the-art solver in Section VI.

## V. PROPOSED ALGORITHM FOR SCHEDULING/PLACEMENT OF HETEROGENEOUS ITS INFRASTRUCTURE

In this section, we propose an algorithm that we developed for placement of ITS infrastructure, as well as daily scheduling. The proposed algorithm is motivated by high complexity associated with solving the model developed in Section IV. The algorithm is a reductive greedy algorithm, working backwards from the busiest time period  $|\mathcal{T}| - 1$  backwards to 0. The intuition behind this stems from the fact that the busiest time periods have a higher likelihood of more traffic, accidents, and other system disruptions. The algorithm has two phases.

### A. Initialization Phase

First, the algorithm computes the importance metric

$$I_t = \frac{\sum_{k \in \Phi} f_{kt}}{\sum_{k \in \Phi} \sum_{T \in \mathcal{T}} f_{kt}} \quad (27)$$

for each time period—which is just simply a set of weights based on the fitness scores in each time period. The algorithm then multiplies each time period's importance metric by the budget to calculate what should be the budget per time period. The algorithm populates each candidate placement location  $j$  with the best-quality RSU of type  $|\mathcal{I}| - 1$  attached to solar panels and computes the coverage efficiency and the budget of the considered installation. If the user prefers UAV installations,

they may set the algorithm to populate each point  $j$  with  $N_b$  UAVs instead. After we initialize with all candidate locations receiving RSU's and solar panels, we must prune this initial coverage by reducing the overlapped infrastructure. We calculate the coverage efficiency for this initial configuration. We then determine the goal coverage efficiency for our pruning process. In our examples in the next section, we set this to be the initial coverage efficiency, i.e., remove redundant RSUs until any loss in coverage efficiency. The excess coverage pruning process proceeds as follows. First, we calculate the average number of overlaps per point for each RSU. This is calculated by determining the number of RSUs that cover each point by the RSU and dividing it by the number of covered points by the RSU. For example, if there were three points covered by an RSU, where each point was covered by one, two, and three RSUs, respectively, then the average number of overlaps per point for that RSU would be  $\frac{1+2+3}{3} = 2$ . After computing this metric for each RSU, we then select the RSU with the maximum overlap matrix, remove it along with its solar panel configuration, and recalculate the RSU configuration's new coverage efficiency, repeating until any actual loss in coverage efficiency.

### B. Runtime Phase

If the calculated budget exceeds the budget, the algorithm will reduce the transmission power of each at point  $j$ , keeping the reduction that minimizes loss to the coverage efficiency. In this time period, if the transmission power goes below the max power threshold of an RSU of a lower tier ( $P_{i-1}^{\max}$ ), the RSU at that location will be replaced with the lower tier RSU. If the transmission power drops below 0, the RSU is replaced with a UAV station with  $N_b$  UAVs. The reduction process is to reduce the UAV station by one UAV. If the user had the UAV preference selected, then the UAV incrementation steps would occur first, and UAV stations would be replaced with a type 2 RSU with a transmission power setting of  $P_2^{\max}$ , then followed with the RSU reduction steps highlighted previously. In this time period, if even the UAV station is reduced to 0 UAVs (transmission power of 0 W if the UAV preference selected), then no infrastructure is installed at point  $j$ , including solar panels. The algorithm will continue the reduction process in the time period until the costs of the reduced system are under the per-period budget and the number of active UAVs does not exceed the maximum fleet size. In all other time periods except the busiest, the algorithm will not change between different RSU types or to UAV stations—the infrastructure planning step occurs only when the algorithm is at  $t = |T| - 1$ . Instead, the power/number of UAVs will simply be reduced to 0, at which case that would be interpreted as the infrastructure at that point being deactivated. The solar panel will still remain. This ensures that all of the constraints to the problem discussed in Section IV are not violated. A flowchart detailing the program control flow can be found in Fig. 2.

## VI. SELECTED NUMERICAL RESULTS AND DISCUSSION

In this section, we start by presenting the parameters chosen for our initial model run. Then, we discuss our numerical results. After, we perform sensitivity analysis on the model. This is then followed by a brief discussion regarding the comparison of infrastructure placement and scheduling when the scope of the problem is the entire day versus a single time period. We then look at how our heuristic performs in a large-scale problem.

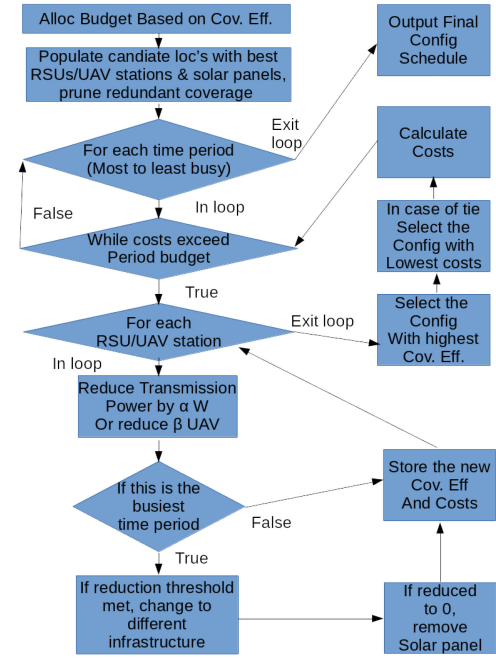


Fig. 2. Program flow diagram for the GRAP (see Algorithm 1).

TABLE I  
INITIAL MODEL RUN PARAMETERS

Parameter	Value	Unit	Parameter	Value	Unit
$ \Phi $	215	N/A	$p_{max,i}, \forall i$	0.1, 0.25, 0.5	W
$ \mathcal{J} $	15	N/A	$f_{kt}, \forall k, t$	[0,1]	Utility
$ \mathcal{T} $	3	N/A	$\gamma$	0.000738	\$/hr
$ \Omega $	1	N/A	$c_{ir}, \forall i$	0.0002, 0.0004, 0.0008	\$/hr
$ \mathcal{I} $	6	N/A	$c_{sg}, \forall q$	0.0002	\$/hr
$R$	6	Mbps	$D$	2.00	\$/6hr
$B$	10	MHz	$\theta_{qt}, \forall q, t$	0, 6, 12, 30, 24, 18	W
$\nu$	3	N/A	$a_i, \forall i$	[8.5, 10, 11.5]	N/A
$S_T$	0.4	N/A	$b_i, \forall i$	[4.25, 5, 5.75]	W
$C_T$	0.4	N/A	$A_d, A_T$	0.3	N/A
$\bar{N}_b$	3	N/A	$p^{use}$	50	Watts
$\delta$	250	meters	$c_d$	0.0001	\$/hr
$\alpha$	0.001	Watts	-	-	-

Finally, we interpret the meaning of the results. When referring to the optimal solution in this section, we are referring to the solution to the single-objective problem formulation.

### A. Data and Parameters

We gather our road network data from the OpenStreetMap project [36], solve a version of the single-objective problem with the Gurobi 8.01 solver that incorporates state-of-the-art algorithms such as branch and bound, model presolve, etc., and use our heuristic to 1) compare to the optimal solution and 2) run a sensitivity analysis on variations of the parameters to test the effectiveness of the heuristic across various situations.

Table I displays the parameters utilized for our initial model run. Recalling the map of Hoboken, NJ in Fig. 1, for tractability, we limit the scope of our optimization to a subset of the points on that map. We utilize this small region (Latitude  $-74.040$ – $-74.030$  and Longitude  $40.740$ – $40.750$ ), with 213 points, due to the NP-hard complexity of solving an MIQCP. Note that our

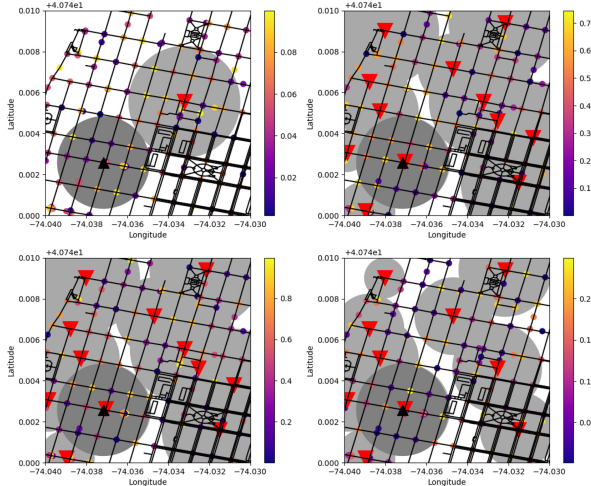


Fig. 3. Visualizing the initial run optimal solution. (Upper left) time period  $t = 0$  ([3 A.M., 7 A.M.] and  $E = 34.9\%$ ), (upper right) time period  $t = 4$  ([7 A.M., 11 A.M.] and  $E = 99.2\%$ ), (lower left) time period  $t = 5$  ([3 P.M., 7 P.M.] and  $E = 99.3\%$ ), and (lower right) time period  $t = 1$  ([11 P.M., 3 A.M.] and  $E = 93.8\%$ ). The light gray circles represent the coverage area of the RSUs, and the dark gray circles represent the coverage of the UAV stations. The one UAV station has three UAVs operating from it.

map has points primarily on intersections—this model would work if points along the stretches of road were also considered.

Since we split the day into six time periods ( $|\mathcal{T}| = 6$ ) of four hours in duration, we use a simplified set of  $\theta_{qt}$  values that reasonably approximate the amount of solar energy generated. We assume that, in the area of interest, there are 15 candidate locations ( $|\mathcal{J}| = 15$ ) to install RSUs of the 215 points ( $|\Phi| = 215$ ) as follows:  $k = 0, 15, 30, 45, \dots, 210$ .

The path loss exponent  $\nu$  is assumed to be 3 [10]. We choose three types of RSUs and one type of solar panel, and we utilize uniform random distributions to generate the fitness values for each time period. The fitness score represents a general concept of how to rate the points based on normalized factors that may be relevant to ITS operators. These factors could be anything from the incidence rate of accidents, to traffic flow, to number of pedestrians, among others, or some combination of all, based on the preferences of the ITS operator. We used random values to simulate how points could potentially be rated and assumed that, in general, the fitness scores would be higher in busier times of the day because, generally, most of the activity occurs during these time periods. The lower and upper bounds, respectively, for each time period are Period 0: [0, 0.1], Period 1: [0, 0.25], Period 2: [0, 0.4], Period 3: [0, 0.6], Period 4: [0, 0.75], and Period 5: [0, 1]. We did not consider real data to score the points, as ITS operators may have different criteria for scoring points based on their objectives.

### B. Initial Model Run Results

In our initial run, we found that the model performed several key tasks. The model will place RSUs and UAV stations based on fitness throughout the day, will deactivate RSUs during less busy parts of the day, will place solar panels, will adjust the transmission power of each RSU to compensate for changes in traffic behavior, and will move UAVs around to maximize their effectiveness based on daily fluctuations.

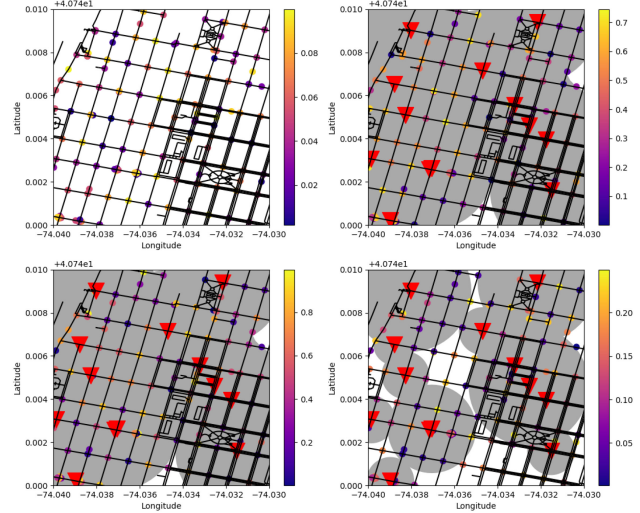


Fig. 4. Visualizing the initial run heuristic solution, where the operator has a preference for RSUs. (Upper left) time period  $t = 0$  ([3 A.M., 7 A.M.] and  $E = 0.0\%$ ), (upper right) time period  $t = 4$  ([7 A.M., 11 A.M.] and  $E = 98.9\%$ ), (lower left) time period  $t = 5$  ([3 P.M., 7 P.M.] and  $E = 99.2\%$ ), and (lower right) time period  $t = 1$  ([11 P.M., 3 A.M.] and  $E = 80.1\%$ ). The light gray circles represent the coverage area of the RSUs.

In Fig. 3, we visualize a selection of the results from the initial run from the Gurobi solver, and in Fig. 4, we visualize the results from the heuristic, given the same parameters, and if the operator prefers UAVs. In the plots, the red triangles represent active RSUs, light gray circles represent the RSU coverage zone, purple to yellow points represent points to be covered, with a darker color corresponding to a lower fitness score, and dark gray circles represent the UAV coverage. The color bar on each figure corresponds to the fitness scores of the points, where as the points get to be a darker blue, the fitness score is decreasing. Figs. 3 (upper left) and 4 (upper left) represent the solution from the late night/early morning time period (for the optimal and heuristic solvers, respectively) ( $t = 0$ ), which has the lowest traffic flow and, therefore, lowest overall fitness score. In the optimal solution run, one RSU and one UAV station are active in this time period. In the heuristic run, no RSUs nor UAV stations are active. Figs. 3 (upper right) and 4 (upper right) represent the morning rush-hour period, which has the second-highest traffic density ( $t = 4$ ). In the optimal solution run, there are 12 active RSUs and one active UAV station, and in the heuristic run, all of the candidate locations have an active RSU and no UAV stations. Figs. 3 (lower left) and 4 (lower left) represent the afternoon/evening rush-hour period, the most active traffic period of the day ( $t = 5$ ), with similar placement/activations as Figs. 3 (upper right) and 4 (upper right). Figs. 3 (lower right) and 4 (lower right) represent the later evening, where traffic density is high, but not as high as the rush-hour period in Figs. 3 (lower left) and 4 (lower left) (e.g.,  $t = 1$ ). To adjust, the RSUs all have their transmission power settings lowered to conserve energy. In  $t = 0$ , there are a lower number of active RSUs in both runs due to the lower fitness scores. The heuristic leaves this time period uncovered due to its emphasis on ensuring that the busier time periods are covered first. As the streets become busier, the other RSUs are activated to adjust for the daily traffic fluctuations. Due to the low amortized CAPEX, every installed RSU has a solar panel attached as well. We also see that while the optimal run installs a UAV station, the heuristic does not, as the optimal

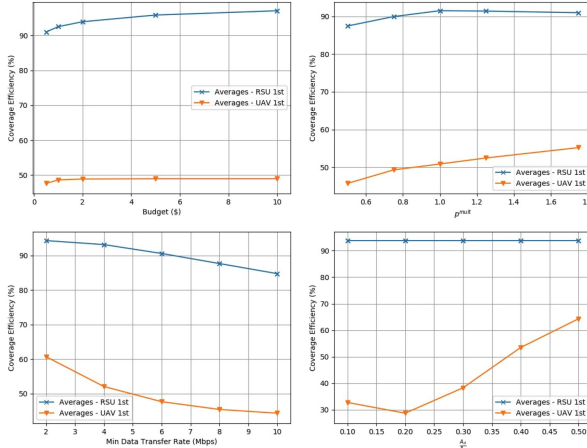


Fig. 5. (Upper left) Financial sensitivity analysis. Positive, monotonic, and diminishing returns relationship between daily coverage efficiency and budget. (Upper right) Sensitivity analysis considering the relationship between  $p^{\text{mult}}$  and coverage efficiency, for low and high budgets, and varying values for the data transmission rate  $R$ . We see that, in general, as the transmission power increases, so does the coverage efficiency. (Lower left) Sensitivity analysis considering the relationship between  $R$  and coverage efficiency, for low and high budgets, and varying values for the power multiplier  $p^{\text{mult}}$ . We see that, in general, as the minimum data throughput requirement increases, the coverage efficiency decreases. (Lower right) Plot of the relationship between the UAV coverage ratio and coverage efficiency.

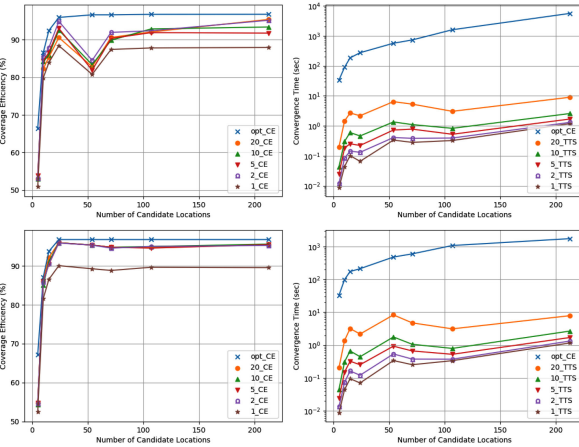


Fig. 6. Plotting complexity (number of candidate locations) versus the coverage efficiency for a low budget (upper left) and high budget (lower left). We see that the worst-case difference between the heuristic and optimal solution is approximately 15% in the low budget scenario, and 10% in the high budget scenario. We also plot complexity versus log-scaled convergence time for a low budget (upper right) and high budget (lower right). We see here that in both cases, the heuristic converges orders of magnitude faster than the off-the-shelf optimizer. As a worst case for the optimizer, this gap in convergence time is over a thousand-fold.

solved for all time periods at once, where the heuristic greedily solved from the higher traffic time period to the lower ones.

### C. Sensitivity Analysis

To test the robustness of the heuristic, we solve the problem with a range of values for  $\bar{D}$ ,  $c_{ir}$ ,  $c_{sq}$ ,  $\gamma$ ,  $R$ ,  $P_i^{\max}$ ,  $\frac{A_d}{A_T}$ ,  $C_T$ ,  $S_T$ , and  $\delta$ , given each potential preference (RSU first or UAV first) by the operator. Fig. 5 (upper left) focuses on the effects of the

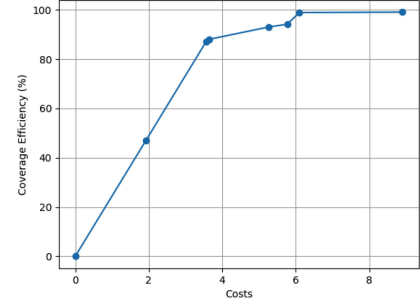


Fig. 7. Plotting the tradeoff between cost and coverage efficiency.

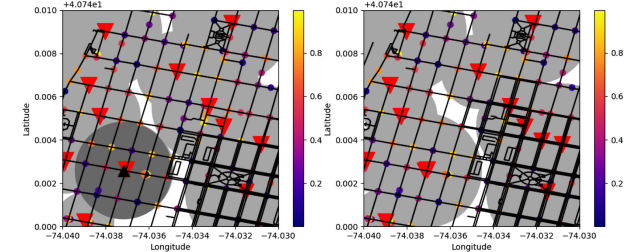


Fig. 8. Comparison of how infrastructure is placed for our initial run parameters given that (left) we optimize for the whole day at one, and (right) if we only optimize for period  $t = 5$ . We obtain the costs of the time period  $t = 5$  installation from the results of optimizing for the whole day and utilize that as the budget for the single-period optimization. Both scenarios result in a 99.3% coverage efficiency. A UAV station is placed in the scenario for the whole day, in order to improve coverage in time period  $t = 0$ , showing the effect of the other time periods on the peak traffic time placement. The gray circles represent the coverage area of the RSUs, and the yellow circles represent the coverage of the UAV stations.

entire day coverage efficiency versus the financial parameters. To simplify the sensitivity analysis, we assume that a type 1 RSU is twice as expensive as a type 0, a type 2 RSU is twice as expensive as a type 1 RSU, a solar panel costs the same as a type 0 RSU to install, and the UAV stations have half the installation costs as a type 0 RSU. We introduce another parameter  $c_m$ , which represents the CAPEX multiplier. For example, consider that, in our initial run,  $c_m = 0.0002$ . From this CAPEX, multiplier, and the previous cost relationships, we came up with the following relationships:

$$c_{ir} = \begin{cases} c_m, & \text{if } i = 0 \\ 2c_m, & \text{if } i = 1 \\ 4c_m, & \text{otherwise} \end{cases} \quad (28)$$

$$c_sq = c_m \quad (29)$$

$$c_d = \frac{c_m}{2}. \quad (30)$$

In our financial parameter sensitivity analysis, we consider the coverage efficiency versus budget given eight combinations of  $c_m$  and  $\gamma$ . The upper left plane in Fig. 5 shows that on average for both cases, there is a general diminishing return effect (e.g., as the budget increases, in general, so should the coverage efficiency; however, the increased gains are smaller as the budget increases), an expected result. We also find that as the per-period expenses in either category increase, the diminishing return behavior becomes less pronounced, further corroborating

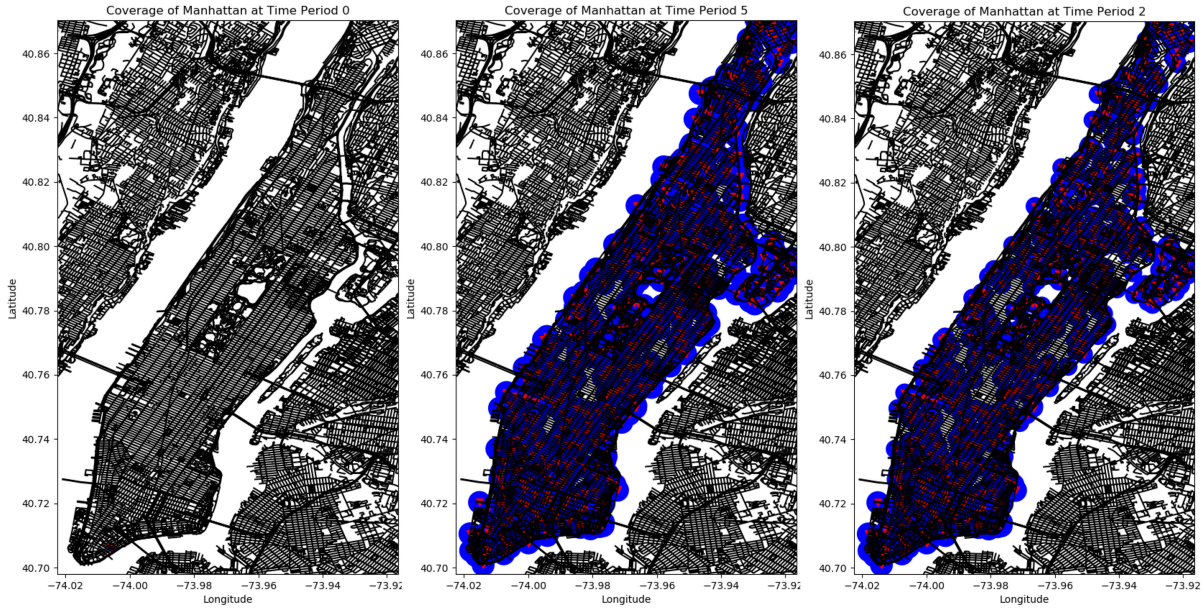


Fig. 9. Visualizing the RSU-first heuristic solution performance for a large-scale problem in Manhattan, New York City, NY, USA. (Left) Time period  $t = 0$  ([3 A.M., 7 A.M.] and  $E = 0.2\%$ ), (middle) time period  $t = 5$  ([3 P.M., 7 P.M.] and  $E = 97.6\%$ ), and (right) time period  $t = 2$  ([7 P.M., 11 P.M.] and  $E = 91.1\%$ ). The blue circles represent the coverage area of the RSUs. The coverage efficiency for the whole day is  $E = 88.7\%$ .

the expected result. In general, for a very wide range of financial parameters, the model will produce a tractable result. The RSU preference selection on the heuristic leads to better results than the UAV preference.

Similar to how we simplified analysis of the CAPEX, we simplified analysis of the  $P_i^{\max}$  values by utilizing a multiplier  $p^{\text{mult}}$ , based on the following relationship:

$$P_i^{\max} = \begin{cases} \frac{1}{10}p^{\text{mult}}, & \text{if } i = 0 \\ \frac{1}{4}p^{\text{mult}}, & \text{if } i = 1 \\ \frac{1}{2}p^{\text{mult}}, & \text{otherwise.} \end{cases} \quad (31)$$

In our initial run,  $p^{\text{mult}} = 1$ . In our RSU technical parameter sensitivity analysis, we consider the relationship between  $p^{\text{mult}}$  versus the daily coverage efficiency, given variations in the budget and the minimum data transfer rate  $R$  to consider the connection to be stable (see Fig. 5), as well as the relationship between  $R$  and the daily coverage efficiency given variations in budget and  $p^{\text{mult}}$  [see Fig. 5 (upper right)].

In Fig. 5 (upper right), we see that on average, as  $p^{\text{mult}}$  increased, so did the coverage efficiency, matching our findings in [1]. This is a result from the positive association between transmission power and transmitter range. As the range increased as a result of increased power, so did the number of points, and therefore, the coverage efficiency. Fig. 5 (lower left) shows that as the minimum required data throughput  $R$  increased, the coverage efficiency decreased, matching our results from [1]. This results from the negative association between minimum throughput and transmitter range.

In our UAV technical parameter sensitivity analysis, we consider the relationship between the ratio  $\frac{A_d}{A_T}$  (the ratio between the UAV's transmitter range and the coverage area of the UAV station's range) and the coverage efficiency, given different combinations of the UAV service time ratio ( $S_T$ ) and the effective

range of the UAV station  $\delta$ . Another way to interpret  $\delta$  is the battery life of the UAV—a larger value for  $\delta$  corresponds to a longer battery life, because UAVs can fly out farther from the station, considering a constant  $S_T$ . In Fig. 5 (lower right), we see no change in the coverage efficiency—this results from the heuristic with the RSU preference setting, as the heuristic exclusively places RSUs in all tested scenarios. In the case of the UAV preference, as the ratio increases, the coverage efficiency increases on average.

#### D. Comparison of Optimal and Heuristic Solutions

In order to gage the effectiveness of the GRAP heuristic, we devised a simplified problem space with one RSU type considered ( $\mathcal{I} = 1$  and  $p_1^{\max} = 0.35$  W) to determine how the optimal and heuristic solutions and the time required for algorithm convergence differed. We ran our experiments on a compute server running Ubuntu Linux version 18.04 running on an Intel Xeon E5-2698 v3, 32-core CPU, rated at an average clock speed of 2.30 GHz per core. Based on Fig. 6, we see that the heuristic at worst finds solutions around 5–10% of the optimal solution, while converging hundreds to thousands of times faster than the state-of-the-art solver. In addition, our implementation of the heuristic was primarily single threaded with some speedup through the numerical python library numpy [37], versus the fully parallelized implementation of the Gurobi solver, which is designed to take advantage of all of the computer's CPU cores in parallel, meaning that if our heuristic was more efficiently implemented, it would have an even more dramatic convergence time savings versus the state-of-the-art optimizer.

#### E. Pareto Frontier Analysis

In this subsection, we solve the multiobjective optimization problem for various values of  $\omega_p$  in order to visualize the Pareto

frontier of this problem as shown in Fig. 7. We see from the figure that the coverage efficiency increases with costs, and that there is a diminishing return relationship between these values.

#### F. Discussion of Results

Our numerical results show that the model is feasible for almost every combination of financial parameters, which directly correspond to the coverage, as a larger budget does correlate with more overall coverage. We also found a diminishing return effect in the financial sensitivity analysis, showing that after a certain point, the benefits of increased financial input into the system become negligible. The technical parameter analysis showed that the maximum power ratings for RSUs and minimum data transfer requirements will affect how effective the system coverage is. Another interesting finding is the sudden increase of the rate of change of increase in financial scenarios with lower marginal operating costs—implying that the change in financial parameters causes the heuristic to find a different local optimum.

After considering how variation of model parameters would affect the results of our model, we look at how considering the whole day at once may result in somewhat unintuitive results for the optimization model. Fig. 8 compares the performance of the optimal solution for the whole day (left) versus performance if we ran the optimization model for only time period 5 (right), due to the redundancy of the UAV station coverage and placement of an RSU at a location. The placement of the UAV station to ensure better coverage in the earlier part of the day results in this. While the costs and coverage efficiency remain the same, the UAV station is a result of better coverage for the earlier time period.

We then proceed to run our heuristic on a large-scale problem—for Manhattan island, with 40 times more points to cover and candidate locations than the small-scale problem. Fig. 9 visualizes how the algorithm behaves in this setting, with the same values for all of the aforementioned parameters in the initial model run except for  $|\mathcal{J}|$  and  $|\mathcal{K}|$ . The red triangles represent placed RSUs, and the yellow circles represent their coverage. We test the heuristic on Manhattan to show that the algorithm does indeed have the capability of solving this problem on very large scales. In order to speed up the solution time, some parts of the algorithm may be parallelized in order to improve performance on large-scale settings.

## VII. CONCLUSION

In this article, we proposed a solution framework for optimal energy-efficient RSU/UAV deployment and daily scheduling—an MIQCP capable of determining an optimal planning solution for heterogeneous ITS infrastructure installation and scheduling, and a fast heuristic that can provide a reasonable solution to the planning problem in a short period of time. Then, we looked at a subset of possible combinations of parameters that could influence the decision provided by it. Additionally, we demonstrated the ability for the heuristic to operate on a large-scale setting in Manhattan. This proposed framework provides ITS planners the ability to consider budget, time variation in traffic, renewable energy, RSU scheduling, and UAV fleet management all at once, helping simplify a highly complex decision for planners. The planning approach presented in this article is for the long-term deployment of heterogeneous ITS infrastructure, which can then

be followed by algorithms that handle more short-term problems, such as resource allocation, UAV job/routing management, dynamic coverage shifting, and data management. Placement of ITS infrastructure in a road network is only the first step, as, moving forward, this system can provide the basis for two directions of research. The first would be a system for the daily UAV management for real-time ITS applications of UAV traffic, and the second would be the development of automated crowdsourcing systems that will aim to improve transportation infrastructure utilization, aid in improvement of disruption response, and propagate useful information back to end-users.

## REFERENCES

- [1] M. C. Lucic, H. Ghazzai, and Y. Massoud, “A generalized and dynamic framework for solar-powered roadside transmitter unit planning,” in *Proc IEEE Int. Syst. Conf.*, Orlando, FL, USA, Apr. 2019, pp. 1–7.
- [2] A. M. Vengi and V. Loscri, “A survey on vehicular social networks,” *IEEE Commun. Surv. Tuts*, vol. 17, no. 4, pp. 2397–2419, Jul. 2015.
- [3] L. Zhu, F. R. Yu, Y. Wang, B. Ning, and T. Tang, “Big data analytics in intelligent transportation systems: A survey,” *IEEE Trans. Intell. Transp. Syst.*, vol. 20, no. 1, pp. 383–398, Jan. 2019.
- [4] Y. Liu, “Big data technology and its analysis of application in urban intelligent transportation system,” in *Proc. Int. Conf. Intell. Transp., Big Data, Smart City*, Xiamen, China, Apr. 2018, pp. 17–19.
- [5] H. Menouar, I. Guvenc, K. Akkaya, A. S. Uluagac, A. Kadri, and A. Tuncer, “UAV-enabled intelligent transportation systems for the smart city: Applications and challenges,” *IEEE Commun. Mag.*, vol. 55, no. 3, pp. 22–28, Mar. 2017.
- [6] K. Lin, C. Li, G. Fortino, and J. J. P. C. Rodrigues, “Vehicle route selection based on game evolution in social internet of vehicles,” *IEEE Internet Things J.*, vol. 5, no. 4, pp. 2423–2430, 2018.
- [7] V. Loscri, G. Ruggeri, A. M. Vigni, and I. Cricelli, “Social structure analysis in Internet of vehicles,” in *Proc. IEEE Int. Conf. Sens. Commun. Netw.*, 2018, pp. 1–4.
- [8] B. Ying and A. Nayak, “Social location privacy protection method in vehicular social networks,” in *Proc. IEEE Int. Conf. Commun. Workshops*, 2017, pp. 1288–1292.
- [9] J. B. Kenney, “Dedicated short-range communications (DSRC) standards in the united states,” *Proc. IEEE*, vol. 99, no. 7, pp. 1162–1182, Jul. 2011.
- [10] T. S. Rappaport, F. Gutierrez, E. Ben-Dor, J. N. Murdock, Y. Qiao, and J. I. Tamir, “Broadband millimeter-wave propagation measurements and models using adaptive-beam antennas for outdoor urban cellular communications,” *IEEE Trans. Antennas Propag.*, vol. 61, no. 4, pp. 1850–1859, Apr. 2013.
- [11] Y. Cao, N. Wang, G. Kamel, and Y. Kim, “An electric vehicle charging management scheme based on publish/subscribe communication framework,” *IEEE Syst. J.*, vol. 11, no. 3, pp. 1822–1835, Sep. 2017.
- [12] Z. Wang, J. Zheng, Y. Wu, and N. Mitton, “A centrality-based RSU deployment approach for vehicular ad hoc networks,” in *Proc. IEEE Int. Conf. Commun.*, Paris, France, May 2017, pp. 1–5.
- [13] C. M. Silva, W. Meira, and J. F. M. Sarubbi, “Non-intrusive planning the roadside infrastructure for vehicular networks,” *IEEE Trans. Intell. Transp. Syst.*, vol. 17, no. 4, pp. 938–947, Apr. 2016.
- [14] N. M. Balouchzahi, M. Fathy, and A. Akbari, “Optimal road side units placement model based on binary integer programming for efficient traffic information advertisement and discovery in vehicular environment,” *IET Trans. Intell. Transp. Syst.*, vol. 9, no. 9, pp. 851–861, Sep. 2015.
- [15] N. Nikookaran, G. Karakostas, and T. D. Todd, “Combining capital and operating expenditure costs in vehicular roadside unit placement,” *IEEE Trans. Veh. Technol.*, vol. 66, no. 8, pp. 7317–7331, Aug. 2017.
- [16] D. C. Vageesh, M. Patra, and C. S. R. Murthy, “Joint placement and sleep scheduling of grid-connected solar powered road side units in vehicular networks,” in *Proc. 12th Int. Symp. Model. Optim. Mobile, Ad Hoc, Wireless Netw.*, Hammamet, Tunisia, May 2014, pp. 534–540.
- [17] M. Fogue, J. Sanguesa, J. Martinez, and J. M. Marquez-Barja, “Improving roadside unit deployment in vehicular networks by exploiting genetic algorithms,” *Appl. Sci.*, vol. 8, no. 1, Jan. 2018, Art. no. 86.
- [18] F. Mohammed, A. Idries, N. Mohammed, J. Al-Jaroodi, and I. Jawhar, “UAVs for smart cities: Opportunities and challenges,” in *Proc. IEEE Int. Conf. Unmanned Aircr. Syst.*, Orlando, FL, USA, May 2014, pp. 267–273.

- [19] M. Elloumi, R. Dhaou, B. Escrig, H. Idoudi, and L. A. Saidane, "Monitoring road traffic with a UAV-based system," in *Proc. IEEE Wireless Commun. Netw. Conf.*, Barcelona, Spain, Apr. 2018, pp. 1–6.
- [20] R. Ke, Z. Li, J. Tang, Z. Pan, and Y. Wang, "Real-time traffic flow parameter estimation from UAV video based on ensemble classifier and optical flow," *IEEE Trans. Intell. Transp. Syst.*, vol. 20, no. 1, pp. 54–64, Jan. 2019.
- [21] L. Xiao, X. Lu, D. Xu, Y. Tang, L. Wang, and W. Zhuang, "UAV relay in VANETs against smart jamming with reinforcement learning," *IEEE Trans. Veh. Technol.*, vol. 67, no. 5, pp. 4087–4097, May 2018.
- [22] S. Mignardi, C. Buratti, A. Bazzi, and R. Verdone, "Trajectories and resource management of flying base stations for C-V2X," *Sensors*, vol. 19, 2019, Art. no. E811.
- [23] H. Binol, E. Bulut, K. Akkaya, and I. Guvenc, "Time optimal multi-UAV path planning for gathering its data from roadside units," in *Proc. IEEE 88th Veh. Technol. Conf.*, Chicago, IL, USA, Aug. 2018, pp. 1–5.
- [24] H. Ghazzai, H. Menouar, A. Kadri, and Y. Massoud, "Future UAV-based ITS: A comprehensive scheduling framework," *IEEE Access*, vol. 7, pp. 75678–75695, 2019.
- [25] H. Ghazzai, H. Menouar, and A. Kadri, "On the placement of UAV docking stations for future intelligent transportation systems," in *Proc. 85th IEEE Veh. Technol. Conf.*, Sydney, NSW, Australia, Jun. 2017, pp. 1–6.
- [26] M. B. Ghorbel, D. Rodriguez-Duarte, H. Ghazzai, M. J. Hossain, and H. Menouar, "Joint position and travel path optimization for energy efficient wireless data gathering using unmanned aerial vehicles," *IEEE Trans. Veh. Technol.*, vol. 68, no. 3, pp. 2165–2175, Mar. 2019.
- [27] H. Ghazzai, A. Kadri, M. B. Ghorbel, H. Menouar, and Y. Massoud, "A generic spatiotemporal UAV scheduling framework for multi-event applications," *IEEE Access*, vol. 7, pp. 215–229, 2018.
- [28] A. V. Savkin and H. Huang, "A method for optimized deployment of a network of surveillance aerial drones," *IEEE Syst. J.*, vol. 13, no. 4, pp. 4474–4477, Dec. 2019.
- [29] G. A. Audu, S. Bhattacharya, and J. M. H. Elmirghani, "Wind energy dependent rate adaptation for roadside units," in *Proc. 9th Int. Conf. Next Gener. Mobile Appl., Services, Technol.*, Cambridge, U.K., Sep. 2015, pp. 156–160.
- [30] W. Wajda, G. Auer, P. Skillermak, Y. Jading, "Energy efficiency analysis of the reference systems, areas of improvement and target breakdown," Tech. Rep. INFSO-ICT-247733 EARTH, Jan. 2012.
- [31] M. B. Brahim, H. Ghazzai, H. Menouar, and F. Filali, "UAVs-assisted data collection in vehicular network," in *Proc. Int. Conf. Adv. Veh. Syst., Technol. Appl.*, Venice, Italy, Jun. 2018, pp. 39–46.
- [32] M. Farooq, H. Ghazzai, A. Kadri, H. ElSawy, and M. Alouini, "A hybrid energy sharing framework for green cellular networks," *IEEE Trans. Commun.*, vol. 65, no. 2, pp. 918–934, Dec. 2018.
- [33] I. Griva, S. G. Nash, and A. Sofer, *Linear and Nonlinear Optimization*, 2nd ed. Philadelphia, PA, USA: SIAM, 2008.
- [34] M. B. Brahim, W. Drira, and F. Filali, "Roadside units placement within city-scaled area in vehicular ad-hoc networks," in *Proc. IEEE Int. Conf. Connected Veh. Expo.*, Vienna, Austria, Nov. 2014, pp. 1010–1016.
- [35] *Gurobi Solver 8.01* [Software], Gurobi Optimization, Inc., Houston, TX, USA, 2018.
- [36] Openstreetmap. [Online]. Available: <https://www.openstreetmap.org>. Accessed on: Jul. 20, 2018.
- [37] T. E. Oliphant, *A Guide to NumPy*. USA: Trelgol Publishing, 2006. [Online]. Available: <https://www.scipy.org/citing.html>



**Michael C. Lucic** (Student Member, IEEE) received the B.Sc. degree in industrial and systems engineering from the University of Florida, Gainesville, FL, USA, in 2018. He is currently working toward the Ph.D. degree with the School of Systems and Enterprises, Stevens Institute of Technology, Hoboken, NJ, USA.

His research interests include data fusion, applied optimization, intelligent transportation systems, smart cities, and applied machine learning.



**Hakim Ghazzai** (Member, IEEE) received the Diplome d'Ingenieur (Hons.) in telecommunication engineering, the master's degree in high-rate transmission systems from the Ecole Supérieure des Communications de Tunis, Tunis, Tunisia, in 2010 and 2011, respectively, and the Ph.D. degree in electrical engineering from the King Abdullah University of Science and Technology, Thuwal, Saudi Arabia, in 2015.

He was a Visiting Researcher with Karlstad University, Karlstad, Sweden, and a Research Scientist with the Qatar Mobility Innovations Center, Doha, Qatar, from 2015 to 2018. He is currently a Research Scientist with the Stevens Institute of Technology, Hoboken, NJ, USA. His general research interests include the intersection of wireless networks, unmanned aerial vehicles, the Internet of Things, intelligent transportation systems, and optimization.

Dr. Ghazzai has been on the Editorial Board of the IEEE COMMUNICATIONS LETTERS and the IEEE Open Journal of the Communications Society since 2019.



**Yehia Massoud** (Fellow, IEEE) received the Ph.D. degree in electrical engineering and computer science from the Massachusetts Institute of Technology (MIT), Cambridge, MA, USA, in 1999.

He is currently the Dean of the School of Systems and Enterprises, Stevens University of Science and Technology, Hoboken, NJ, USA. He has authored more than 280 articles in peer-reviewed journals and conferences. He has held several academic and industrial positions, including a member of the technical staff with the Advanced Technology Group, Synopsys, Inc., CA, USA, a Tenured Faculty with the Department of Electrical and Computer Engineering and the Department of Computer Science, Rice University, Houston, TX, USA, the W. R. Bunn Head of the Department of Electrical and Computer Engineering, The University of Alabama, Birmingham, AL, USA, and the Head of the Department of Electrical and Computer Engineering, Worcester Polytechnic Institute, Worcester, MA, USA.

Dr. Massoud has served as a Distinguished Lecturer by the IEEE Circuits and Systems Society and as an Elected Member of the IEEE Nanotechnology Council. He was selected as one of the ten MIT Alumni Featured by MIT's Electrical Engineering and Computer Science Department in 2012. He was a recipient of the Rising Star of Texas Medal in 2007, the National Science Foundation CAREER Award in 2005, the DAC Fellowship in 2005, the Synopsys Special Recognition Engineering Award in 2000, several best paper award nominations, and two best paper awards at the 2007 IEEE International Symposium on Quality Electronic Design and the 2011 IEEE International Conference on Nanotechnology. He has served as an Editor for *Mixed-Signal Letters—The Americas* and as an Associate Editor for the IEEE TRANSACTIONS ON VERY LARGE SCALE INTEGRATION SYSTEMS and the IEEE TRANSACTIONS ON CIRCUITS AND SYSTEMS I: REGULAR PAPERS.